ACS APPLIED MATERIALS & INTERFACES

Research Article

www.acsami.org

Facile and Environmentally Friendly Solution-Processed Aluminum Oxide Dielectric for Low-Temperature, High-Performance Oxide Thin-Film Transistors

Wangying Xu,[†] Han Wang,[†] Fangyan Xie,[‡] Jian Chen,[‡] Hongtao Cao,[*,§] and Jian-Bin Xu[*,†]

[†]Department of Electronic Engineering, Materials Science and Technology Research Center, The Chinese University of Hong Kong (CUHK), Shatin, New Territories, Hong Kong, China

[‡]Instrumental Analysis & Research Center, Sun Yat-Sen (Zhongshan) University, Guangzhou, China

[§]Division of Functional Materials and Nano Devices, Ningbo Institute of Materials Technology & Engineering (NIMTE), Chinese Academy of Sciences, Ningbo, China

Supporting Information

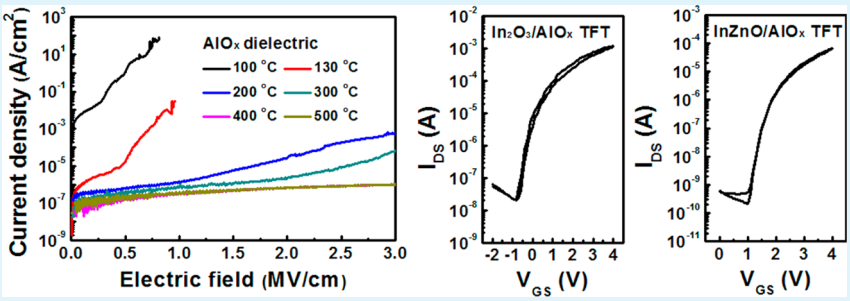

ABSTRACT: We developed a facile and environmentally friendly solution-processed method for aluminum oxide (AlO_x) dielectrics. The formation and properties of AlO_x thin films under various annealing temperatures were intensively investigated by thermogravimetric analysis−differential scanning calorimetry (TGA-DSC), X-ray diffraction (XRD), spectroscopic ellipsometry, atomic force microscopy (AFM), attenuated total reflectance−Fourier transform infrared spectroscopy (ATR-FTIR), X-ray photoelectron spectroscopy (XPS), impedance spectroscopy, and leakage current measurements. The sol−gel-derived AlO_x thin film undergoes the decomposition of organic residuals and nitrate groups, as well as conversion of aluminum hydroxides to form aluminum oxide, as the annealing temperature increases. Finally, the AlO_x film is used as gate dielectric for a variety of low-temperature solution-processed oxide TFTs. Above all, the In_2O_3 and InZnO TFTs exhibited high average mobilities of 57.2 $cm^2\ V^{-1}\ s^{-1}$ and 10.1 $cm^2\ V^{-1}\ s^{-1}$, as well as an on/off current ratio of ~10^5 and low operating voltages of 4 V at a maximum processing temperature of 300 °C. Therefore, the solution-processable AlO_x could be a promising candidate dielectric for low-cost, low-temperature, and high-performance oxide electronics.

KEYWORDS: *solution process, aluminum oxide, oxide thin-film transistors, environmentally friendly, low-temperature, high-performance*

1. INTRODUCTION

Metal oxide thin-film transistors (TFTs) have been extensively studied for large-area flat-panel display applications over the past decade, because of their high mobility, good uniformity, and reasonable electrical stability.[1−6] Unfortunately, most of these high-performance oxide TFTs are usually manufactured using costly vacuum-based techniques. To address this problem, much effort has been devoted to fabricating TFTs using alternative deposition methods based on solution-processed oxide semiconductors.[7−12]

However, most of the reported work employs thermally grown or vacuum-deposited SiO_2 dielectrics. The development of dielectrics by solution processing is somewhat overlooked, even though the dielectric layer is as important as the semiconductor layer and the semiconductor/dielectric interface strongly affects the device performance. The development of novel dielectrics that offer solution processing capability is an important objective for the realization of low-cost oxide-based electronics. For this reason, a few studies have investigated solution-processed high-*k* dielectrics, such as Al_2O_3, HfO_2, ZrO_2 and Y_2O_3.[13−39] Among them, Al_2O_3 is an excellent candidate, because of its abundance in nature, low cost, good chemical stability, high breakdown field, and low interfacial trap density with oxide semiconductors.[14,29,40,41] However, the high annealing temperature, repeated spin-coating processes (usually more than 5 times), or the use of hazardous solvent still inhibit

Received: December 12, 2014
Accepted: February 13, 2015
Published: February 13, 2015

ACS Publications © 2015 American Chemical Society

DOI: 10.1021/am508775c
ACS Appl. Mater. Interfaces 2015, 7, 5803−5810

the development of solution-processed high-k Al_2O_3 dielectrics.[26,28,30,32−36,39]

In this article, a simple and environmentally friendly method is developed for AlO_x dielectric using ethanol as solvent in a single spin-coating process. The formation and properties of AlO_x thin films at different annealing temperatures were intensively studied by thermogravimetric analysis−differential scanning calorimetry (TGA-DSC), X-ray diffraction (XRD), spectroscopic ellipsometry, atomic force microscopy (AFM), attenuated total reflectance−Fourier transform infrared spectroscopy (ATR-FTIR), X-ray photoelectron microscopy (XPS), impedance spectroscopy, and leakage current measurements. The AlO_x film exhibited a low leakage current and smooth surface, which is used as a gate dielectric for a variety of low-temperature solution-processed oxide TFTs. Above all, the In_2O_3 and InZnO TFTs showed high average mobilities of 57.2 $cm^2\ V^{-1}\ s^{-1}$ and 10.1 $cm^2\ V^{-1}\ s^{-1}$, as well as on/off current ratios of $\sim 10^5$ and low operating voltages of 4 V, with a maximum processing temperature of 300 °C.

2. EXPERIMENTAL SECTION

2.1. Precursor Solution Synthesis. All of the chemical compounds were purchased from Sigma−Aldrich and used without further purification. The AlO_x precursor solution was prepared by dissolving ∼4.5 g of aluminum nitrate nonahydrate ($Al(NO_3)_3{\cdot}9H_2O$) in 20 mL of ethanol (an environmentally friendly solvent) without any additives. For the In_2O_3 solution, 0.15 M indium nitrate hydrate ($In(NO_3)_3{\cdot}xH_2O$) was dissolved in 2-methoxyethanol (2-ME). For the InZnO solution, 0.08 M indium nitrate hydrate ($In(NO_3)_3{\cdot}xH_2O$) and 0.08 M zinc acetate dihydrate ($Zn(CH_3COO)_2{\cdot}2H_2O$) were mixed with 2-ME. All the solutions were stirred vigorously for 6 h under ambient conditions and filtered through 0.2 μm polytetrafluoroethylene (PTFE) syringe filters, respectively, before spin-coating.

2.2. Device Fabrications. The gate dielectric and channel layers were all achieved by single spin-coating processes. The AlO_x precursor solution was spin-coated onto an oxygen-plasma-treated heavily doped Si substrate at 4000 rpm for 40 s and annealed at the desired temperature (100, 130, 200, 300, 400, and 500 °C) for 30 min under ambient conditions. For the metal−insulator−metal (MIM) devices, an Al electrode (100 nm) was deposited on the dielectric layer by thermal evaporation. The area of the circular Al electrode was 0.03 mm^2. To fabricate the TFTs with a bottom-gate top-contact configuration, the semiconductor solutions (In_2O_3 and InZnO) were spin-coated on AlO_x (annealed at 300 °C) coated heavily doped Si substrate at a speed of 3500 rpm for 35 s, respectively. The coated In_2O_3 and InZnO layers were annealed at the intended temperature (250 and 300 °C) for 50 min. The thickness of the channel layers were 10 nm, as measured using a spectroscopic ellipsometer. Subsequently, the Al source and drain electrodes 100 nm thick were deposited by thermal evaporation through the shadow mask to fabricate top-contact transistors. The channel width (W) and length (L) are 1500 and 100 μm, respectively. It has been reported that a small W/L ratio of 5 may induce mobility overestimation up to ∼200%, whereas the overestimation decreased to 10% as the W/L ratio increased to 10.[26] Herein, the large W/L ratio of >15 in this work could efficiently limit mobility overestimation.

2.3. Characterization. The thermal behavior of the AlO_x precursor powder, which was dried at 100 °C for 12 h, was measured by thermogravimetric analyzer (Perkin−Elmer, Model TGA 6) and differential scanning calorimeter (Perkin−Elmer, Model DSC 7) at a heating rate of 10 °C/min from 50 °C to 500 °C. The crystallization and structural information on the sol−gel-derived AlO_x thin films were obtained using X-ray diffraction (XRD) (Siemens, Model D5005) with Cu Kα radiation. The thicknesses of the AlO_x films were measured via variable-angle spectroscopic ellipsometry (SE) (J.A. Woollam Co., Inc.). The surface morphologies of the AlO_x films were observed by atomic force microscopy (AFM) (Veeco Dimention V). The chemical characteristics of the AlO_x films were investigated by attenuated total reflectance−Fourier transform infrared spectroscopy (ATR-FTIR) (Bruker, Model Tensor 27). The chemical structures of the AlO_x films were characterized by X-ray photoelectron spectroscopy (XPS) (VG Scientific, Model ESCALAB 250), and all binding energies were referenced to the C 1s peak at 284.6 eV of the surface adventitious carbon. Impedance spectroscopy measurements on MIM devices were performed using a Model HP 4284A precision impedance analyzer at frequencies between 20 Hz and 1 MHz. The leakage of the AlO_x films and the electrical characteristics of the TFTs were measured with a precision semiconductor analyzer (Keithley, Model 4200) in the dark at room temperature. The threshold voltage (V_{th}) was extracted from measurements in the saturation region by plotting $(I_{DS})^{1/2}$ vs V_{GS} and extrapolating to $I_{DS} = 0$ plots. The mobility (μ) and subthreshold swing (S) were calculated using the following formulas:

$$I_{DS} = \left(\frac{\mu C_i W}{2L}\right)(V_{GS} - V_{th})^2$$

$$S = \left(\frac{d(\log_{10} I_{DS})}{dV_{GS}}\right)^{-1}$$

where C_i is the capacitance of the gate dielectrics per unit area, W the channel width, and L the channel length.

3. RESULTS AND DISCUSSION

To understand the conversion process from liquid precursor to solid AlO_x thin film, systematical investigations including TGA-DSC, XRD, SE, AFM, ATR-FTIR, and XPS characterization were carried out. Figure 1 shows the TGA-DSC of AlO_x precursor powder from 50 °C to 500 °C. Gradually weight loss was observed up to 400 °C. The endothermic peak accompanying weight loss at 133 °C can be attributed to the evaporation of solvent and hydrolysis of the metal precursors.[20,33,42] The peak at 209 °C indicates the dehydroxylation

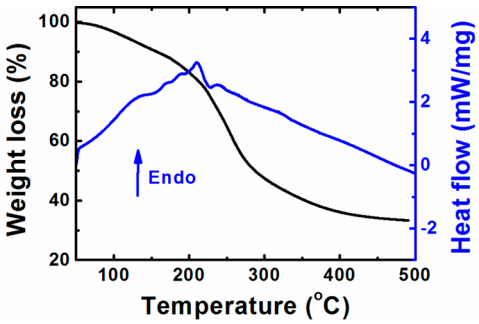

Figure 1. TG and DSC curves of AlO_x precursor powder from 50 °C to 500 °C.

DOI: 10.1021/am508775c
ACS Appl. Mater. Interfaces 2015, 7, 5803−5810

Table 1. Microstructural and Dielectric Properties of Solution-Processed AlO_x at the Different Annealing Temperatures of 100, 130, 200, 300, 400, and 500 °C

annealing temperature (°C)	thickness (nm)	roughness (nm)	Leakage (A/cm^2) at 1 MV/cm	Leakage (A/cm^2) at 3 MV/cm	capacitance (nF/cm^2) at 100 Hz	dielectric constant at 100 Hz	dissipation factor at 100 Hz
100	151	2.38	79.6	>79.6	920	157.0	4.8×10^{-1}
130	89	1.33	3.1×10^{-2}	$>3.1 \times 10^{-2}$	1110	111.6	1.6×10^{-1}
200	56	0.17	1.4×10^{-6}	5.7×10^{-4}	241	15.2	6.6×10^{-2}
300	52	0.15	7.1×10^{-7}	6.4×10^{-5}	194	11.4	2.2×10^{-2}
400	51	0.14	3.2×10^{-7}	1.0×10^{-6}	170	9.8	6.7×10^{-3}
500	47	0.16	4.1×10^{-7}	9.8×10^{-7}	163	8.7	6.6×10^{-3}

behavior of the hydrolyzed aluminum hydroxide, which reacts with adjacent aluminum hydroxide molecules and form the aluminum oxide clusters.[20,33,42] Another peak at 238 °C may be related to the decomposition of residual nitrate.[20,33,42]

Figure S1 in the Supporting Information shows the XRD spectra of AlO_x films at the different annealing temperature of 100, 130, 200, 300, 400, and 500 °C. The AlO_x film was identified as an amorphous phase up to the annealing temperature of 500 °C. Previous studies have demonstrated that the AlO_x thin film showed high crystallization temperature up to 1000 °C.[41] Concerning the structures, amorphous materials are preferred, because grain boundaries act as preferential paths for impurity diffusion and leakage current, resulting in inferior dielectric performance. Besides that, amorphous films present smoother surfaces than polycrystalline ones, which can render improved dielectric/channel interface properties.[31]

The thicknesses of AlO_x films annealed at 100, 130, 200, 300, 400, and 500 °C were 151, 89, 56, 52, 51, and 47 nm, respectively, as summarized in Table 1. As the annealing temperature increased, the thickness of AlO_x thin film decreased, which is due to the evaporation of solvent and the densification process of the thin films. Figure 2 shows the AFM images (5 μm × 5 μm) of AlO_x thin films treated at different temperatures. The root-mean-square (rms) roughness of AlO_x films annealed at 100, 130, 200, 300, 400, and 500 °C were 2.38, 1.33, 0.17, 0.15, 0.14, and 0.16 nm, respectively (see Table 1). The AlO_x films showed an ultrasmooth surface as the annealing temperature increased, up to 200 °C, consistent with the amorphous structure, which is ideal for suppressing the surface-roughness-induced leakage current and achieving expeditious charge carrier mobility in the TFT channel.[21,26,31] The thickness and surface roughness of AlO_x films were greatly reduced when the annealing temperature increased to 200 °C, which is consistent with the TGA-DSC measurements. Besides, the AlO_x films maintain excellent surface roughness up to annealing temperatures of 500 °C.

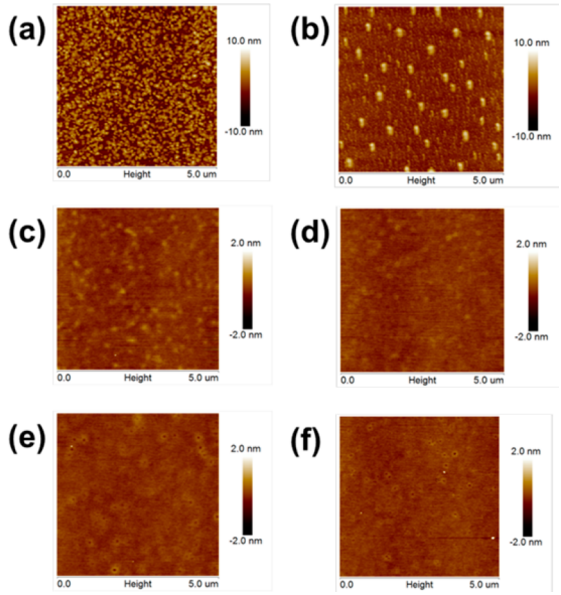

Figure 2. AFM images of AlO_x films at different annealing temperatures of (a) 100, (b) 130, (c) 200, (d) 300, (e) 400, and (f) 500 °C. Image dimensions are 5 μm × 5 μm.

To investigate the formation of the solution-processed AlO_x thin films with aforementioned annealing conditions, ATR-FTIR measurements were carried out, and the results are shown in Figure 3. The broad peaks in the range of 3000−3500 cm^{-1} correspond to hydroxyl (OH) groups stretching vibrations.[20,33] The peaks in the 1300−1700 cm^{-1} range indicate deformation vibrations from the nitrate (NO_3^-) groups.[33] The peaks in the 600−900 cm^{-1} range are attributed to Al−O vibrations.[43] The peaks at 1240 cm^{-1} (with annealing temperature reaching above 200 °C) could be related to the substrate information (Si−O−Si (native oxide) vibrations),[44,45] whereas it could not be detected for thick film. In the case of 100 °C annealed conditions, the Al−O bond was not formed and a large amount of hydroxyl and nitrate groups remained. The Al−O bond was configured at 200 °C and the hydroxyl and nitrate groups gradually decomposed at temperatures up to 300 °C. At annealing temperatures of >400 °C, only Al−O vibration peaks were observed.

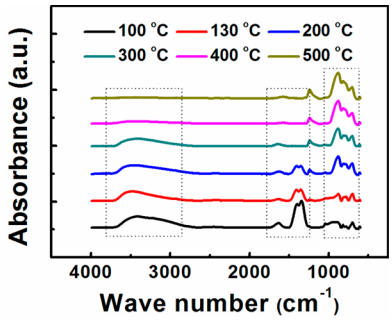

Figure 3. FTIR spectra of AlO_x films at different annealing temperatures.

To further investigate the evolution of solution-processed AlO_x thin film, XPS measurements were performed. The XPS O 1s peaks of the AlO_x films that were prepared at different annealing temperatures are shown in Figure 4. They can be deconvoluted into two peaks, corresponding to the fully

DOI: 10.1021/am508775c
ACS Appl. Mater. Interfaces 2015, 7, 5803−5810

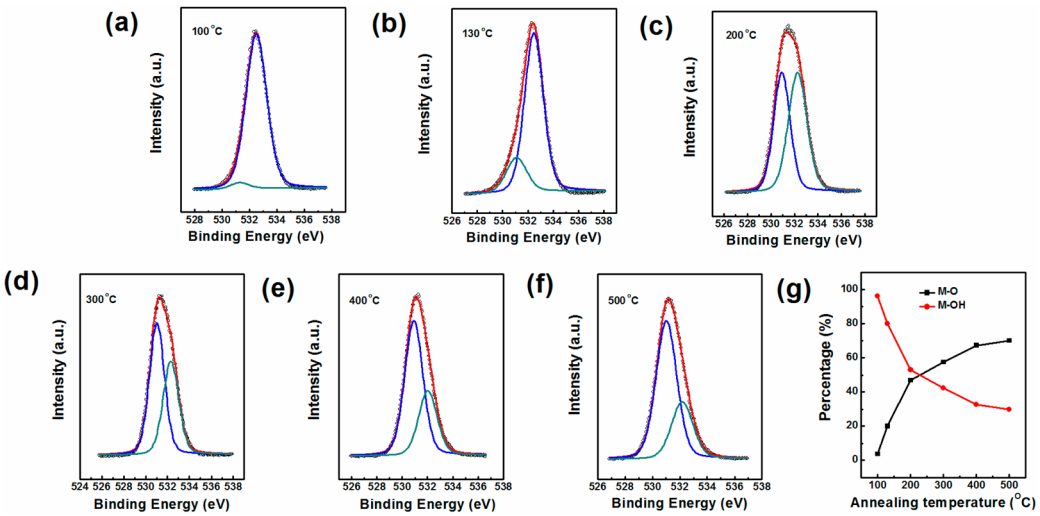

Figure 4. XPS spectra of AlO_x films at different annealing temperatures of (a) 100, (b) 130, (c) 200, (d) 300, (e) 400, and (f) 500 °C. The open circles represent the experimental data, while the solid lines are the fitted peaks. (g) Percentage of oxide lattices and oxygen in hydroxide of AlO_x films.

oxidized states at 531.0 ± 0.1 eV and the oxygen associated with hydroxyl (OH) group at 532.3 ± 0.2 eV.[29,46] As shown in Figure 5g, the oxygen lattice and OH-related peaks of the AlO_x film increased and decreased as the annealing temperature increased, suggesting decomposition of the metal precursor and conversion of the hydroxyl groups to form a metal oxide framework. Besides, a large number of nitrogen peaks were observed in the 100 °C-annealed AlO_x film, whereas nitrogen could not be detected when the annealing temperature up to 300 °C, which is consistent with the ATR-FTIR analysis. From the TGA-DSC, ATR-FTIR, and XPS results, we can conclude that the sol−gel-derived AlO_x thin film undergoes the decomposition of organic residuals and nitrate groups, as well as conversion of aluminum hydroxides to form aluminum oxide, as the annealing temperature increases. The proposed mechanism of the conversion process from liquid precursor to solid AlO_x thin film was demonstrated in S1.

The dielectric properties of the solution-processed AlO_x thin film annealed at different temperatures were measured by MIM structures and summarized in Table 1. Figure 5 shows the current density versus electric field of AlO_x films, as a function of annealing temperature. It is clearly seen that the leakage current of the AlO_x thin films decreased as the annealing temperature increased. The 100 °C- and 130 °C-annealed AlO_x thin films had very large leakage currents, since the existence of large amounts of organic residuals, as well as nitrate and hydroxyl groups, will lead to the conduction paths.[20,31] The 200 °C- and 300 °C-annealed films showed significant improvement in the leakage current (1.4×10^{-6} A/cm^2 and 7.1×10^{-7} A/cm^2, respectively, at 1 MV/cm, and 5.7×10^{-4} A/cm^2 and 6.4×10^{-5} A/cm^2, respectively, at 3 MV/cm), which is attributed to the decomposition of metal precursor, as well as the formation of a metal oxide framework.[20,31] These results show that the low-temperature solution-processed AlO_x dielectric layer is suitable for use in gate dielectrics for TFT applications. Besides, the leakage current is smaller than the previously published results of sol−gel-derived AlO_x dielectrics.[26,29,33,36,39] As the annealing temperature increased to 400 °C and 500 °C, the leakage current further reduced to 3.2×10^{-7} A/cm^2 and 4.1×10^{-7} A/cm^2 at 1 MV/cm, and 1.0×10^{-6} A/cm^2 and 9.8×10^{-7} A/cm^2, respectively, at 3 MV/cm, which is ascribed to the continued conversion of aluminum hydroxides to form aluminum oxide.[29]

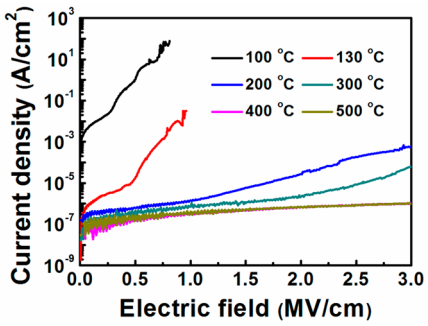

Figure 5. Leakage current density versus electric field of AlO_x films at different annealing temperatures. The 400 °C- and 500 °C-annealed curves are overlapped with each other.

The capacitance−frequency and dissipation factor−frequency curves of AlO_x thin films are shown in Figure 6 in the range from 20 Hz to 1 MHz. The 100 °C- and 130 °C-annealed AlO_x films exhibited anomalous capacitances and dissipation factors because of the organic residuals, which is consistent with the poor leakage current. The films annealed at 200, 300, 400, and 500 °C had capacitances of 241, 194, 170, and 163 nF/cm^2 at 100 Hz, corresponding to dielectric constants of 15.2, 11.4, 9.8, and 8.7, respectively. The high value of capacitance in the case of low-temperature-annealed AlO_x films is attributed to the existence of hydroxyl groups. In general, hydroxyl groups easily absorb water molecules, which can enhance the capacitance of the AlO_x layer, because of their high polarity (the dielectric constant of water is 81).[29,33] The dissipation factor of the films annealed at 200, 300, 400, and 500 °C were 6.6×10^{-2}, 2.2×10^{-2}, 6.7×10^{-3}, and 6.6×10^{-3}, respectively. The reduced dissipation factor is consistent with the low leakage current and weak frequency dependence of capacitance.[27,38] The dielectric properties and leakage current are in good agreement with the above characterization of the AlO_x thin film.

DOI: 10.1021/am508775c
ACS Appl. Mater. Interfaces 2015, 7, 5803−5810

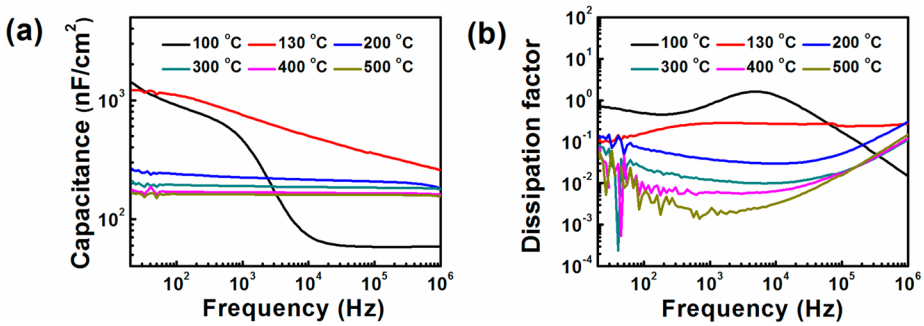

Figure 6. (a) Capacitance versus frequency and (b) dissipation factor versus frequency of AlO_x films at the different annealing temperatures.

Table 2. Electrical Performance of Oxide TFTs with Solution-Processed AlO_x Dielectric

channel material	mobility(cm^2 V^{-1} s^{-1})	subthreshold swing (V/decade)	threshold voltage (V)	on/off current ratio
In_2O_3 (250 °C)	1.71 ± 0.78	0.29 ± 0.04	−1.13 ± 1.02	1.1×10^4
In_2O_3 (300 °C)	57.21 ± 16.91	0.22 ± 0.05	0.57 ± 0.67	6.0×10^4
InZnO (250 °C)	1.20 ± 0.23	0.29 ± 0.14	1.56 ± 0.50	1.4×10^4
InZnO (300 °C)	10.13 ± 2.86	0.17 ± 0.06	2.07 ± 0.42	2.9×10^5

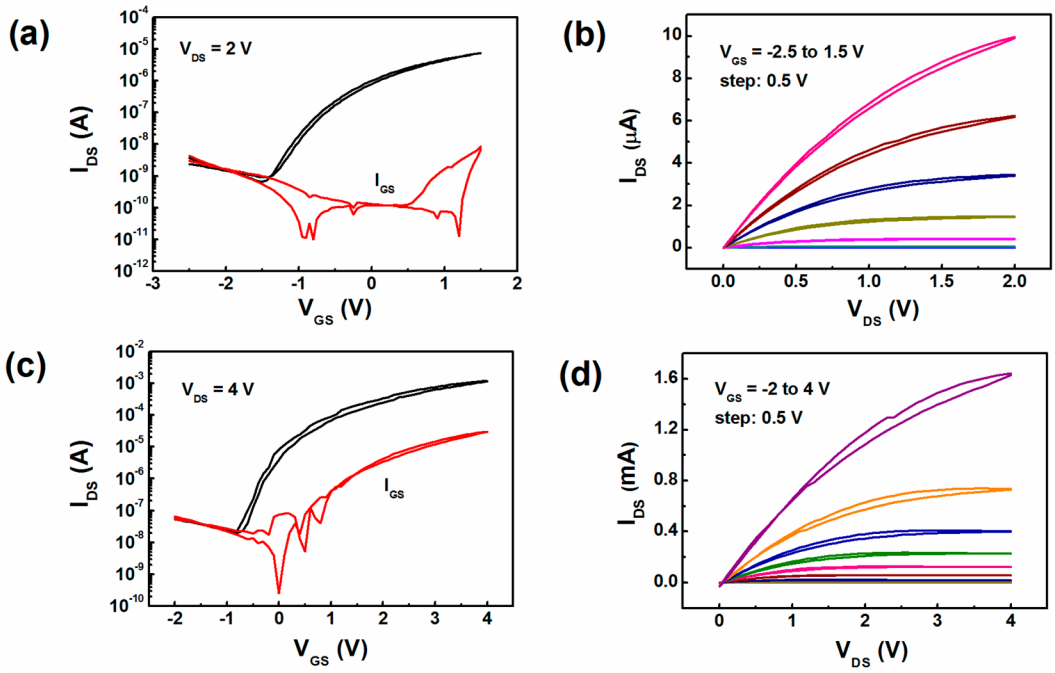

Figure 7. (a) Transfer (I_{DS} vs V_{GS})/gate leakage (I_{GS} vs V_{GS}) and (b) output characteristics of the In_2O_3/AlO_x TFTs annealed at 250 °C. (c) Transfer (I_{DS} vs V_{GS})/gate leakage (I_{GS} vs V_{GS}) and (d) output characteristics of the In_2O_3/AlO_x TFTs annealed at 300 °C.

In order to avoid the miscibility phenomenon caused by the annealing treatment of oxide semiconductors (such as indium diffusion) and to guarantee a low-temperature process, we conducted the annealing process for AlO_x dielectric at 300 °C for oxide TFTs.[24] The performance of the AlO_x thin film as a gate dielectric was investigated in a bottom-gate, top-contact TFTs architecture employing solution-processed In_2O_3 and InZnO as channel layers, with the electrical performance summarized in Table 2.

Figure 7 shows the representative transfer and output characteristics of solution-processed In_2O_3 annealed at 250 and 300 °C with AlO_x dielectrics. No evidence of current crowding appears for the low V_{DS} of the output curves, indicating good ohmic contacts between the semiconductor and the source−drain electrodes, and the contact resistance does not limit the device performance.[31] Because TFT characterization was performed in direct voltage, the measured capacitance value at a relatively low frequency was often adopted for device mobility calculation. Therefore, the capacitance at 20 Hz was used to eliminate mobility overestimation.[26,33] The In_2O_3 TFT annealed at 250 °C exhibited a mobility of 1.71 ± 0.78 cm^2 V^{-1} s^{-1}, a subthreshold swing of 0.29 ± 0.04 V/decade, a threshold voltage of −1.13 ± 1.02 V, and an on/off current ratio of 1.1×10^4. A remarkable improvement is achieved for the 300 °C-annealed device, showing a high mobility of 57.21 ± 16.91 cm^2 V^{-1} s^{-1}, a subthreshold swing of 0.22 ± 0.05 V/decade, a threshold voltage of 0.57 ± 0.67 V, and an on/off current ratio of 6.0×10^4. The histograms of these parameters are shown in Figure S2 in the Supporting Information. It is known that the conduction

DOI: 10.1021/am508775c
ACS Appl. Mater. Interfaces 2015, 7, 5803−5810

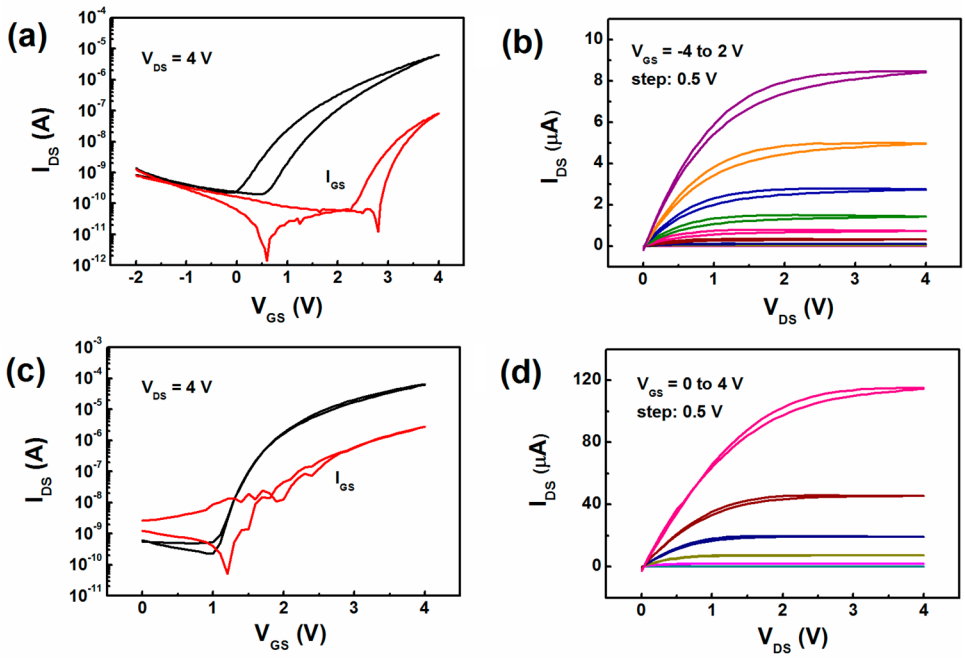

Figure 8. (a) Transfer (I_{DS} vs V_{GS})/gate leakage (I_{GS} vs V_{GS}) and (b) output characteristics of the InZnO/AlO_x TFTs annealed at 250 °C. (c) Transfer (I_{DS} vs V_{GS})/gate leakage (I_{GS} vs V_{GS}) and (d) output characteristics of the InZnO/AlO_x TFTs annealed at 300 °C.

band minimum (CBM) in oxide semiconductors should be primarily composed of dispersed vacant s-states with short interaction distances for efficient carrier transport, which can be achieved in ionic oxide lattices but not obviously in hydroxide.[47] Therefore, the dehydroxylation reaction of oxide semiconductor at higher annealing temperature will enhance the device performance. Besides, the In_2O_3/AlO_x TFTs exhibited a low operating voltage of 4 V, which is good for low power consumption. The relatively high gate leakage current of the device is ascribed to the nonpatterned channel layer, which is consistent with the previous reports.[26,31] However, the device performance is not affected by the gate leakage current, since the leakage current is lower than the drain current by at least a factor of 100.[21,47] The high mobility of the optimized In_2O_3 TFTs should be attributed to the combined effect of a high-quality active layer, a high capacitance dielectric layer, and a well-defined dielectric/semiconductor interface (low interface roughness and trap density).[26,29,31] This high mobility, which is achieved by a simple and low-temperature process, is comparable to the recently reported high-performance solution-processed high-*k* dielectric/oxide semiconductor TFTs.[13,14,16,18−21,24,26−29,33]

InZnO TFTs were also fabricated, again to highlight the applications of solution-processed AlO_x dielectrics. The transfer and output characteristics of InZnO TFTs annealed at 250 and 300 °C are presented in Figure 8. The 250 °C-annealed device showed a mobility of 1.20 ± 0.23 $cm^2\ V^{-1}\ s^{-1}$, a subthreshold swing of 0.29 ± 0.14 V/decade, a threshold voltage of 1.56 ± 0.50 V, and an on/off current ratio of 1.4×10^4. As in the case of the In_2O_3 semiconductor, the 300 °C-annealed InZnO TFT showed an improved mobility of 10.13 ± 2.86 $cm^2\ V^{-1}\ s^{-1}$, a subthreshold swing of 0.17 ± 0.06 V/decade, a threshold voltage of 2.07 ± 0.42 V, and on/off current ratio of 2.9×10^5. The histograms of these parameters are shown in Figure S3 in the Supporting Information. The carrier concentration of In_2O_3 thin films is known to be easily controlled through the addition of different-sized metal cations, such as Zn and Ga, which leads to the reduction of mobility and off current, as well as the positive shift of the threshold voltage.[11,31]

Our results showed that the solution-processed AlO_x is a general dielectric that can be used to achieve low-temperature, high-performance oxide TFTs. We noticed clockwise hysteresis for the 250 °C-annealed In_2O_3 and InZnO TFTs and small counterclockwise hysteresis for the 300 °C-annealed devices. The hysteresis may be related to the charge trapping/detrapping behavior at the semiconductor/dielectric interface.[1,2,4] Besides, since our device is unpassivated, the interaction between the back channel and the ambient atmosphere will contribute to the hysteresis of the device.[3,8] The reduction of the hysteresis and improvement of the device stability could be achieved by optimization of the semiconductor/dielectric interface and the introduction of the passivation layer; related studies are underway. Besides, the annealing temperature (300 °C) is still somewhat high for a flexible substrate. The electrical performance of our device fabricated at low temperature is largely limited by the channel layer. Since the oxide semiconductor is obtained using the conventional sol−gel method, the high-annealing step is inevitable for oxidation and impurity removal in the solution process. Further reduction in the annealing temperature could be achieved by using some novel methods such as sol−gel on chip,[10] combustion process,[9] aqueous solution process,[48] photochemical activation,[11] and annealing in an O_2/O_3 atmosphere environment.[49]

4. CONCLUSION

In summary, we demonstrated a simple and environmentally friendly solution-processed method for AlO_x dielectrics. The formation and properties of AlO_x thin films under various annealing temperatures were intensively studied using TG-DSC, XRD, spectroscopic ellipsometry, AFM, ATR-FTIR, XPS, impedance spectroscopy, and leakage current measurements. As the post-annealing temperature increased, the solution-processed AlO_x thin film undergoes the decomposition of

DOI: 10.1021/am508775c
ACS Appl. Mater. Interfaces 2015, 7, 5803−5810

organic residuals and nitrate groups, as well as conversion of aluminum hydroxides to form aluminum oxide. Finally, the AlO_x film is used as a gate dielectric for a variety of low-temperature solution-processed oxide TFTs. Above all, the In_2O_3 and InZnO TFTs exhibited high average mobilities of 57.2 $cm^2 V^{-1} s^{-1}$ and 10.1 $cm^2 V^{-1} s^{-1}$, as well as an on/off current ratio of $\sim 10^5$ and low operating voltages of 4 V at a maximum processing temperature of 300 °C. Our study presents a significant step toward the development of low-cost, low-temperature, and high-performance oxide electronics.

■ ASSOCIATED CONTENT

Supporting Information

Schematic descriptions and the analyses of the formation of the AlO_x thin film, XRD spectra of AlO_x films at different annealing temperatures, and the histograms of electrical parameters for In_2O_3 and InZnO TFTs. This material is available free of charge via the Internet at http://pubs.acs.org.

■ AUTHOR INFORMATION

Corresponding Authors

*E-mail: h_cao@nimte.ac.cn (H. Cao).
*E-mail: jbxu@ee.cuhk.edu.hk (J.-B. Xu).

Notes

The authors declare no competing financial interest.

■ ACKNOWLEDGMENTS

We thank Dr. Danqing Liu (CUHK), Dr. Lingyan Liang and Mr. Hao Luo (NIMTE) for experimental help and discussions. The work is in part supported by the Research Grants Council of Hong Kong, particularly, via Grant No. AoE/P-03/08, No. CUHK4179/10E, No. N_CUHK405/12, and the CUHK Group Research Scheme. J. B. Xu would like to thank the National Science Foundation of China for the support, particularly, via Grant No. 61229401.

■ REFERENCES

(1) Fortunato, E.; Barquinha, P.; Martins, R. Oxide Semiconductor Thin-Film Transistors: A Review of Recent Advances. *Adv. Mater.* **2012**, *24*, 2945−2986.

(2) Park, J. S.; Maeng, W.-J.; Kim, H.-S.; Park, J.-S. Review of Recent Developments in Amorphous Oxide Semiconductor Thin-Film Transistor Devices. *Thin Solid Films* **2012**, *520*, 1679−1693.

(3) Jeong, J. K. The Status and Perspectives of Metal Oxide Thin-Film Transistors for Active Matrix Flexible Displays. *Semicond. Sci. Technol.* **2011**, *26*, 034008.

(4) Xu, W.; Dai, M.; Liang, L.; Liu, Z.; Sun, X.; Wan, Q.; Cao, H. Anomalous Bias-Stress-Induced Unstable Phenomena of InZnO Thin-Film Transistors Using Ta_2O_5 Gate Dielectric. *J. Phys. D: Appl. Phys.* **2012**, *45*, 205103.

(5) Dai, M. Z.; Xu, W. Y. Polarization Mechanism and Quasi-Electric-Double-Layer Modeling for Indium-Tin-Oxide Electric-Double-Layer Thin-Film-Transistors. *Appl. Phys. Lett.* **2012**, *100*, 113506.

(6) Nomura, K.; Ohta, H.; Takagi, A.; Kamiya, T.; Hirano, M.; Hosono, H. Room-Temperature Fabrication of Transparent Flexible Thin-Film Transistors Using Amorphous Oxide Semiconductors. *Nature* **2004**, *432*, 488−492.

(7) Jeong, S.; Moon, J. Low-Temperature, Solution-Processed Metal Oxide Thin Film Transistors. *J. Mater. Chem.* **2012**, *22*, 1243−1250.

(8) Xu, W.; Liu, D.; Wang, H.; Ye, L.; Miao, Q.; Xu, J.-B. Facile Passivation of Solution-Processed InZnO Thin-Film Transistors by Octadecylphosphonic Acid Self-Assembled Monolayers at Room Temperature. *Appl. Phys. Lett.* **2014**, *104*, 173504.

(9) Kim, M. G.; Kanatzidis, M. G.; Facchetti, A.; Marks, T. J. Low-Temperature Fabrication of High-Performance Metal Oxide Thin-Film Electronics Via Combustion Processing. *Nat. Mater.* **2011**, *10*, 382−388.

(10) Banger, K. K.; Yamashita, Y.; Mori, K.; Peterson, R. L.; Leedham, T.; Rickard, J.; Sirringhaus, H. Low-Temperature, High-Performance Solution-Processed Metal Oxide Thin-Film Transistors Formed by a "Sol−Gel on Chip" Process. *Nat. Mater.* **2011**, *10*, 45−50.

(11) Kim, Y. H.; Heo, J. S.; Kim, T. H.; Park, S.; Yoon, M. H.; Kim, J.; Oh, M. S.; Yi, G. R.; Noh, Y. Y.; Park, S. K. Flexible Metal-Oxide Devices Made by Room-Temperature Photochemical Activation of Sol−Gel Films. *Nature* **2012**, *489*, 128−U191.

(12) Thomas, S. R.; Pattanasattayavong, P.; Anthopoulos, T. D. Solution-Processable Metal Oxide Semiconductors for Thin-Film Transistor Applications. *Chem. Soc. Rev.* **2013**, *42*, 6910−6923.

(13) Adamopoulos, G.; Thomas, S.; Wobkenberg, P. H.; Bradley, D. D.; McLachlan, M. A.; Anthopoulos, T. D. High-Mobility Low-Voltage ZnO and Li-Doped ZnO Transistors Based on ZrO_2 High-*k* Dielectric Grown by Spray Pyrolysis in Ambient Air. *Adv. Mater.* **2011**, *23*, 1894−1898.

(14) Avis, C.; Jang, J. High-Performance Solution Processed Oxide TFT with Aluminum Oxide Gate Dielectric Fabricated by a Sol-Gel Method. *J. Mater. Chem.* **2011**, *21*, 10649−10652.

(15) Avis, C.; Kim, Y. G.; Jang, J. Solution Processed Hafnium Oxide as a Gate Insulator for Low-Voltage Oxide Thin-Film Transistors. *J. Mater. Chem.* **2012**, *22*, 17415−17420.

(16) Song, K.; Yang, W.; Jung, Y.; Jeong, S.; Moon, J. A Solution-Processed Yttrium Oxide Gate Insulator for High-Performance All-Solution-Processed Fully Transparent Thin Film Transistors. *J. Mater. Chem.* **2012**, *22*, 21265−21271.

(17) Ha, T.-J.; Dodabalapur, A. Photo Stability of Solution-Processed Low-Voltage High Mobility Zinc-Tin-Oxide/ZrO_2 Thin-Film Transistors for Transparent Display Applications. *Appl. Phys. Lett.* **2013**, *102*, 123506.

(18) Jang, J.; Kitsomboonloha, R.; Swisher, S. L.; Park, E. S.; Kang, H.; Subramanian, V. Transparent High-Performance Thin Film Transistors from Solution-Processed SnO_2/ZrO_2 Gel-like Precursors. *Adv. Mater.* **2013**, *25*, 1042−1047.

(19) Park, J. H.; Yoo, Y. B.; Lee, K. H.; Jang, W. S.; Oh, J. Y.; Chae, S. S.; Baik, H. K. Low-Temperature, High-Performance Solution-Processed Thin-Film Transistors with Peroxo-Zirconium Oxide Dielectric. *ACS Appl. Mater. Interfaces* **2013**, *5*, 410−417.

(20) Park, J. H.; Yoo, Y. B.; Lee, K. H.; Jang, W. S.; Oh, J. Y.; Chae, S. S.; Lee, H. W.; Han, S. W.; Baik, H. K. Boron-Doped Peroxo-Zirconium Oxide Dielectric for High-Performance, Low-Temperature, Solution-Processed Indium Oxide Thin-Film Transistor. *ACS Appl. Mater. Interfaces* **2013**, *5*, 8067−8075.

(21) Yang, W.; Song, K.; Jung, Y.; Jeong, S.; Moon, J. Solution-Deposited Zr-Doped AlO_x Gate Dielectrics Enabling High-Performance Flexible Transparent Thin Film Transistors. *J. Mater. Chem. C* **2013**, *1*, 4275−4282.

(22) Yoo, Y. B.; Park, J. H.; Lee, K. H.; Lee, H. W.; Song, K. M.; Lee, S. J.; Baik, H. K. Solution-Processed High-*k* HfO_2 Gate Dielectric Processed under Softening Temperature of Polymer Substrates. *J. Mater. Chem. C* **2013**, *1*, 1651−1658.

(23) Ko, J.; Kim, J.; Park, S. Y.; Lee, E.; Kim, K.; Lim, K.-H.; Kim, Y. S. Solution-Processed Amorphous Hafnium-Lanthanum Oxide Gate Insulator for Oxide Thin-Film Transistors. *J. Mater. Chem. C* **2014**, *2*, 1050−1056.

(24) Liu, A.; Liu, G. X.; Zhu, H. H.; Xu, F.; Fortunato, E.; Martins, R.; Shan, F. K. Fully Solution-Processed Low-Voltage Aqueous In_2O_3 Thin-Film Transistors Using an Ultrathin ZrO_x Dielectric. *ACS Appl. Mater. Interfaces* **2014**, *6*, 17364−17369.

(25) Je, S. Y.; Son, B. G.; Kim, H. G.; Park, M. Y.; Do, L. M.; Choi, R.; Jeong, J. K. Solution-Processable $LaZrO_x/SiO_2$ Gate Dielectric at Low Temperature of 180 °C for High-Performance Metal Oxide Field-Effect Transistors. *ACS Appl. Mater. Interfaces* **2014**, *6*, 18693−18703.

(26) Huang, G.; Duan, L.; Dong, G.; Zhang, D.; Qiu, Y. High-Mobility Solution-Processed Tin Oxide Thin-Film Transistors with

DOI: 10.1021/am508775c
ACS Appl. Mater. Interfaces 2015, 7, 5803−5810

High-Kappa Alumina Dielectric Working in Enhancement Mode. *ACS Appl. Mater. Interfaces* **2014**, *6*, 20786−20794.
(27) Esro, M.; Vourlias, G.; Somerton, C.; Milne, W. I.; Adamopoulos, G. High-Mobility ZnO Thin Film Transistors Based on Solution-Processed Hafnium Oxide Gate Dielectrics. *Adv. Funct. Mater.* **2014**, *25*, 134−141.
(28) Bae, E. J.; Kang, Y. H.; Han, M.; Lee, C.; Cho, S. Y. Soluble Oxide Gate Dielectrics Prepared Using the Self-Combustion Reaction for High-Performance Thin-Film Transistors. *J. Mater. Chem. C* **2014**, *2*, 5695−5703.
(29) Nayak, P. K.; Hedhili, M. N.; Cha, D.; Alshareef, H. N. High Performance In_2O_3 Thin Film Transistors Using Chemically Derived Aluminum Oxide Dielectric. *Appl. Phys. Lett.* **2013**, *103*, 033518.
(30) Ha, H. J.; Jeong, S. W.; Oh, T.-Y.; Kim, M.; Choi, K.; Park, J. H.; Ju, B.-K. Flexible Low-Voltage Pentacene Memory Thin-Film Transistors with Combustion-Processable Al_2O_3 Gate Dielectric and Au Nanoparticles. *J. Phys. D: Appl. Phys.* **2013**, *46*, 235102.
(31) Xu, W.; Wang, H.; Ye, L.; Xu, J. The Role of Solution-Processed High-κ Gate Dielectrics in Electrical Performance of Oxide Thin-Film Transistors. *J. Mater. Chem. C* **2014**, *2*, 5389−5396.
(32) Wang, H.; Sun, T.; Xu, W.; Xie, F.; Ye, L.; Xiao, Y.; Wang, Y.; Chen, J.; Xu, J. Low-Temperature Facile Solution-Processed Gate Dielectric for Combustion Derived Oxide Thin Film Transistors. *RSC Adv.* **2014**, *4*, 54729−54739.
(33) Park, J. H.; Kim, K.; Yoo, Y. B.; Park, S. Y.; Lim, K.-H.; Lee, K. H.; Baik, H. K.; Kim, Y. S. Water Adsorption Effects of Nitrate Ion Coordinated Al_2O_3 Dielectric for High Performance Metal-Oxide Thin-Film Transistor. *J. Mater. Chem. C* **2013**, *1*, 7166−7174.
(34) Meyers, S. T.; Anderson, J. T.; Hong, D.; Hung, C. M.; Wager, J. F.; Keszler, D. A. Solution-Processed Aluminum Oxide Phosphate Thin-Film Dielectrics. *Chem. Mater.* **2007**, *19*, 4023−4029.
(35) Rim, Y. S.; Chen, H. J.; Liu, Y. S.; Bae, S. H.; Kim, H. J.; Yang, Y. Direct Light Pattern Integration of Low-Temperature Solution-Processed All-Oxide Flexible Electronics. *ACS Nano* **2014**, *8*, 9680−9686.
(36) Liu, Y.; Guan, P. F.; Zhang, B.; Falk, M. L.; Katz, H. E. Ion Dependence of Gate Dielectric Behavior of Alkali Metal Ion-Incorporated Aluminas in Oxide Field-Effect Transistors. *Chem. Mater.* **2013**, *25*, 3788−3796.
(37) Xu, X. L.; Cui, Q. Y.; Jin, Y. Z.; Guo, X. J. Low-Voltage Zinc Oxide Thin-Film Transistors with Solution-Processed Channel and Dielectric Layers Below 150 °C. *Appl. Phys. Lett.* **2012**, *101*, 222114.
(38) Adamopoulos, G.; Thomas, S.; Bradley, D. D. C.; McLachlan, M. A.; Anthopoulos, T. D. Low-Voltage ZnO Thin-Film Transistors Based on Y_2O_3 and Al_2O_3 High-*k* Dielectrics Deposited by Spray Pyrolysis in Air. *Appl. Phys. Lett.* **2011**, *98*, 123503.
(39) Branquinho, R.; Salgueiro, D.; Santos, L.; Barquinha, P.; Pereira, L.; Martins, R.; Fortunato, E. Aqueous Combustion Synthesis of Aluminum Oxide Thin Films and Application as Gate Dielectric in GZTO Solution-Based TFTs. *ACS Appl. Mater. Interfaces* **2014**, *6*, 19592−19599.
(40) Liang, L. Y.; Cao, H. T.; Liu, Q.; Jiang, K. M.; Liu, Z. M.; Zhuge, F.; Deng, F. L. Substrate Biasing Effect on the Physical Properties of Reactive Rf-Magnetron-Sputtered Aluminum Oxide Dielectric Films on ITO Glasses. *ACS Appl. Mater. Interfaces* **2014**, *6*, 2255−2261.
(41) Robertson, J. High Dielectric Constant Gate Oxides for Metal Oxide Si Transistors. *Rep. Prog. Phys.* **2006**, *69*, 327−396.
(42) Jun, T.; Jung, Y.; Song, K.; Moon, J. Influences of pH and Ligand Type on the Performance of Inorganic Aqueous Precursor-Derived ZnO Thin Film Transistors. *ACS Appl. Mater. Interfaces* **2011**, *3*, 774−781.
(43) Adamczyk, A.; Dlugon, E. The Ftir Studies of Gels and Thin Films of Al_2O_3−TiO_2 and Al_2O_3−TiO_2−SiO_2 Systems. *Spectrochim. Acta, Part A* **2012**, *89*, 11−17.
(44) Tian, R. H.; Seitz, O.; Li, M.; Hu, W. C.; Chabal, Y. J.; Gao, J. M. Infrared Characterization of Interfacial Si−O Bond Formation on Silanized Flat SiO_2/Si Surfaces. *Langmuir* **2010**, *26*, 4563−4566.
(45) Rouchon, D.; Rochat, N.; Gustavo, F.; Chabli, A.; Renault, O.; Besson, P. Study of Ultrathin Silicon Oxide Films by FTIR-ATR and ARXPS after Wet Chemical Cleaning Processes. *Surf. Interface Anal.* **2002**, *34*, 445−450.
(46) van den Brand, J.; Sloof, W. G.; Terryn, H.; de Wit, J. H. W. Correlation between Hydroxyl Fraction and O/Al Atomic Ratio as Determined from XPS Spectra of Aluminium Oxide Layers. *Surf. Interface Anal.* **2004**, *36*, 81−88.
(47) Jeong, S.; Ha, Y. G.; Moon, J.; Facchetti, A.; Marks, T. J. Role of Gallium Doping in Dramatically Lowering Amorphous-Oxide Processing Temperatures for Solution-Derived Indium Zinc Oxide Thin-Film Transistors. *Adv. Mater.* **2010**, *22*, 1346−1350.
(48) Hwang, Y. H.; Seo, J.-S.; Yun, J. M.; Park, H.; Yang, S.; Park, S.-H. K.; Bae, B.-S. An "Aqueous Route" for the Fabrication of Low-Temperature-Processable Oxide Flexible Transparent Thin-Film Transistors on Plastic Substrates. *NPG Asia Mater.* **2013**, *5*, e45.
(49) Han, S.-Y.; Herman, G. S.; Chang, C. Low-Temperature, High-Performance, Solution-Processed Indium Oxide Thin-Film Transistors. *J. Am. Chem. Soc.* **2011**, *133*, 5166−5169.

DOI: 10.1021/am508775c
ACS Appl. Mater. Interfaces 2015, 7, 5803−5810